LAWRENCE
LIVERMORE
NATIONAL
LABORATORY

LLNL-TR-404630

Nuclear data verification based on Monte Carlo simulations of the LLNL pulsed-sphere benchmark experiments (1979 & 1986) using the Mercury code

M.-A. Descalle, J. Pruet

June 12, 2008

Disclaimer

This work performed under the auspices of the U.S. Department of Energy by Lawrence Livermore National Laboratory under Contract DE-AC52-07NA27344.

Nuclear data verification based on Monte Carlo simulations of the LLNL pulsed-sphere benchmark experiments (1979 & 1986) using the Mercury code

Marie-Anne Descalle and Jason Pruet

Abstract

Livermore's nuclear data group developed a new verification and validation test suite to ensure the quality of data used in application codes. This is based on models of LLNL's pulsed sphere fusion shielding benchmark experiments. Simulations were done with Mercury, a 3D particle transport Monte Carlo code using continuous–energy cross-section libraries. Results were compared to measurements of neutron leakage spectra generated by 14MeV neutrons in 17 target assemblies (for a blank target assembly, H_2O, Teflon, C, N_2, Al, Si, Ti, Fe, Cu, Ta, W, Au, Pb, ^{232}Th, ^{235}U, ^{238}U, and ^{239}Pu). We also tested the fidelity of simulations for photon production associated with neutron interactions in the different materials. Gamma-ray leakage energy per neutron was obtained from a simple 1D spherical geometry assembly and compared to three codes (TART, COG, MCNP5) and several versions of the Evaluated Nuclear Data File (ENDF) and Evaluated Nuclear Data Libraries (ENDL) cross-section libraries. These tests uncovered a number of errors in photon production cross-sections, and were instrumental to the V&V of different cross-section libraries. Development of the pulsed sphere tests also uncovered the need for new Mercury capabilities. To enable simulations of neutron time-of-flight experiments the nuclear data group implemented an improved treatment of biased angular scattering in MCAPM.

1. Background

The nuclear data community relies on extensive set of benchmark experiments, such as criticality or fusion nuclear shielding experiments, to test new evaluations of cross-section databases. One such set came out of the LLNL pulsed-sphere benchmark experiments program. Most reported verification and validation efforts [Marchetti98, Van der Marck06] deal solely with neutrons cross-sections and compare Monte Carlo simulations with benchmark experiments done in the 1970s and early 80's. [Wong72, Hansen79] In this report, with the exception of HEU and Pu-239, we focused on a set of data published in the late 80's where both neutron time-of-flight and gammas production, through electron recoil spectra, were measured in a NE213 detector.[Goldberg90] The chosen target materials are commonly used in the design of fusion and hybrid reactors. These benchmark experiments allow to compare calculations of neutron and gamma-ray leakage spectra to measurements and have already been instrumental in ensuring the quality of existing cross-section databases, as well as in highlighting needed areas of research and necessary re-evaluations.

2. Experimental set-up

The experimental set-up consists of a deuteron beam hitting a tritiated target embedded in a sphere of material. Neutrons time-of-flight (TOF) and gamma spectra are recorded in a NE213 detector.

A 400 keV deuteron beam is focused on a small target made of titanium tritiate, generating a quasi-isotropic source of ~14 MeV neutrons. The target assembly consists of the source placed in an aluminium holder with a tungsten backing. For details and schematics, refer to p.10 of Wong et al. [Wong72]. The target is estimated to be a disk 1.2 cm in diameter. The pulse width has been described as a normal time distribution with mean=0 and sigma=0.4 ns or 2ns depending on the experiment. The target assembly is positioned in such way that the T-Ti target is at the center of the sphere and fit in the sphere through a conical opening.

Two sets of experiments are modeled here. 15 sphere materials were tested and dimensions are given in table 1. Except for the teflon sphere, radii are smaller than 15 cm. There are four sphere designs defined as general, silicon, H2O flask, and dewar vessel filled with liquid nitrogen. Refer to

Goldberg 1990 and Wong 1972 for technical drawings. The authors chose spheres with a thickness of ~30g/cm^2 to maximize the gamma ray leakage per source neutron.
Two older experiments used spheres made of Pu-239 and HEU, with a radius of 3.5 and 3.145 cm respectively. Refer to Hansel79 and Gosnell95 for technical drawings.

The source and the detector were in adjacent rooms separated by a 197 cm-thick concrete wall. A line of sight was provided by an iron collimator with an opening 20.2 cm in diameter. The collimator itself was several inches thick, and surrounded by a water jacket ~ 5ft in diameter. These dimensions were obtained from discussions with Bert Pohl one of the authors (03/13/06). The detector and the collimator were at a 27 degrees angle from the deuteron beam line. The T-Ti target was 512 cm from the collimator face, and the distance from the source to the center of NE213 detector was 852.5cm for most experiments, and 946.46 cm for the Pu-239 and HEU spheres.

The detector was made of NE213, a liquid scintillator of composition C45H55 and density of 0.874 g/cm^3. It was housed in a cylindrical aluminium container capped with a glass window for coupling to the phototube. The cavity was nominally 5.08 cm x 5.08 cm (2"x 2"). The liquid scintillator had a very-low neutron energy bias estimated to be close to 0.8 MeV for the 15 materials and to 1.43 MeV for Pu-239 and HEU.

Several sets of efficiency curves have been published for equivalent neutron energy biases that vary from 0.8 to ~3 MeV. [Wong72, Hansen79, Marchetti98] To model the late 80's experiments we used the detector response that Afredo Marchetti simulated for the low bias of 0.8MeV, for lack of a measured one. For Pu-239 and HEU, we used the NE213 efficiency published by Hansen et al. [Hansen79]

3. Experimental data

Measured data for Pu-239 and HEU were available in the ASCII computer file "disp93in". This file contains data for about 70 experiments, a subset of the measurements obtained by the LLNL pulsed-sphere program over 15 years. For the more recent experiments comprised of the blank run and 15 spheres, measurement data were digitized from Goldberg et al. 1990. This was decided after a phone conversation in April 2007 with Luisa Hansen, one of the PIs of the LLNL pulsed-sphere experiments program, during which she confirmed that the data from the 1986 experiments were lost.

Table I: Spherical Target Assemblies

Material	r [g/cm3]	R1 [cm]	D [cm]	R2 [cm]	A [deg]	d [cm]	Sphere design
Carbon	1.76	10.16	2.26		4	0.131	1
Nitrogen	0.808						3
H2O	1.00						4
C2F4	2.22	16.50	2.84		3.4	0.64	1
Al	2.70	8.94	2.84		3.4	0.64	1
Si	2.33	10.16		1.11		0	2
Ti	4.45	8.94	2.84		3.4	0.64	1
Fe	7.85	4.46	2.22		4	0.475	1
Cu	8.96	4.00	2.55		1.5	0.324	1
Ta	16.6	3.40	2.54		1.5	0.324	1
W	19.3	10.36		7.82		0	2
Au	19.3	6.21	2.54		4	0	1
Pb	11.3	5.56	2.4		3.4	0.34	1

Th232	11.7	5.76	2.22		4	0.475	1
U238	17.8	3.63	2.22		4	0.475	1
U235	18.55	3.15	2.225		4	0.475	1
Pu239	15.8	3.5	2.606		4	0.475	5

4. Simulations

Calculations were obtained with Mercury, a modern multipurpose 3D Monte Carlo particle transport code being developed at LLNL [Mercury06]. We defined a detailed model including the collimation, and a point detector. To test gamma production, we ran 1D spherical geometry calculations.

4.1. Pulse-sphere experiment

The geometry of the model consists of the target assembly, the sphere of material and the detector, plus the thick concrete wall and the details of the collimation. The distance from the source to the center of the detector is 852.5 cm for the more recent experiments, and 946.46 cm for ^{239}Pu and HEU spheres. For fissile materials, the simulations tracked prompt neutrons. The target assembly was modeled in detail, and is included in all simulations. The neutron source is a point source, with a correlated distribution in energy and angle as defined by Marchetti et al. [Marchetti98] The source distribution covers the energy range from 12.4 to 16.0 MeV in 0.1 MeV wide energy bins, while cosine varies from -1 to 1 in 0.1 increment. The source is at a distance of 852.5 cm from the center of the detector.

Spheres were modeled according to specified diagrams and dimensions, with the exception of the lead sphere that was modeled without a thin outer steel shell. Due to the highly collimated configuration of the experiment, the neutron tally was a point detector. The neutron flux was folded with the detector response.

A python script was written to normalize the results and convert energy bin boundaries to time-of-flight, for comparison with measurements. The normalization takes into account Mercury's own quirks: results are given as a function of the total number of source particles, i.e. they are not normalized per source particle; plus for static calculations, the code assigns a Δt of 10^6 s; and it does not report yet information on tally statistics such as the standard deviation and relative error. Results were calculated for 10^8 histories to insure decent statistics.. The normalization is given in equation 1 below:

$$\phi = result_{mercury} * \frac{10^6 s}{\#source \cdot neutrons} * S_0 \quad \text{(eq. 1)}$$

where S_0 is the source strength. The conversion process from energy to TOF is straightforward.

As discussed by Frankle et al., there is a lot of controversy regarding the normalization process. For our purposes, we feel the normalization is appropriate. [Frankle04] When further details resurface, we expect to improve the process.

A few detailed models were also developed for the COG Monte Carlo code to anlalyze differences between measured and simulated neutron TOF spectra, and determine if they were due to code implementation or cross-section libraries. [Lent02]

4.2. Gamma Production

Goldberg et al. published a set of values of γ MeV/n that can be used to validate coupled neutron-photon codes. These values were obtained from 1D TART simulations. The model consists of a point source of 14 MeV neutrons at the center of a sphere of radius R equal to 1 cm and of ρR given in table 2. Gamma ray energy leakage results were tallied for 15 materials and are also shown in Table

2. We reproduced these simulations with several codes and cross-section libraries: 1) MCNP5 and ENDF/B-VI r8, 2) for COG and ENDF/B-VI r7, and 3) Mercury with an early translation of ENDF/B-VII.

5. Results

5.1. Neutron TOF spectra

Comparisons of measured and simulated neutron time-of-flight spectra are presented for several materials in figure 1 to 18, for the ENDF/B-VII.0 cross section library. For all cases except HEU and ^{239}Pu, we can observe a peak around 162 ns (~14.0-14.1 MeV), followed by a long tail up to time around 500 ns. The simulation for the target assembly in air differs significantly from the measured data (fig. 1). The experimental data show a peak at 350 ns as a result of 2.81MeV neutrons generated by the reaction ^{2}H(d,n)^{3}He due to the deuterium build-up in the tritiated target.[Goldberg90] There is excellent agreement between measurements and simulations up to 425 ns for water contained in the pyrex flask, and up to 400 ns for Teflon, two materials with a large hydrogen content that will down scatter neutron efficiently to energies below the detector threshold. Results for iron, U-238, U235 and Pu239 are also in good agreement with the measurements, while for copper, features in the low energy tail are not fully reproduced in the simulated spectrum.

For aluminium, silicon and titanium, the peak areas are in good agreement up to 200 ns. For spheres made of high Z material, namely lead, tungsten and gold, the simulations exhibit a dip in neutrons compared to measurements in the 175 to 200 ns range. For graphite, simulations are greater than measurements by a factor of two in the 220 to 400 ns range, which corresponds to the 7.7 to 4.3 MeV. Finally, results for nitrogen, and tantalum are off, and might point to issues with the neutron cross-sections.

Several factors can account for the discrepancies between measured and simulated TOF spectra, which are:

- Cross-section libraries
- Normalization
- Detector response: simulated versus measured
- Source: correlated distribution, point/disk source, static/time distribution
- Code implementation.

Frankle noted the importance of modeling the concrete wall and collimation, and the target holder, especially for lighter elements. [Frankle04a&b] Some of the discrepancies observed for the blank case could be due to differences between the real and ideal geometry of the target assembly. In Wong's initial report, the schematic of the target assembly is referred to as "idealized" and there are inconsistencies between the dimensions given in the schematic and the mass of material shown in the accompanying table. To explore the effect of the model of the target assembly, we changed the density of some of the materials to more realistic ones, and used the densities defined by Alfredo Marchetti et al.[Marchetti98] We also modified our model to match exactly his model by increasing the thicknesses of the tungsten backstop and the Al-Cu window. These changes had little effects on the spectra. However the presence or absence of the target assembly in the model did have an effect for low Z (graphite) and high Z material (U-235) and we showed that the target assembly contributes to the low energy tail of the TOF spectra.

5.2. Gamma ray leakage

Simulations of gamma ray energy leakage in a simple spherical geometry are presented in Table II. Overall, there is good agreement between our simulations and the older TART simulations, except for water where the ENDF/B-VII results are greater by up to a factor of two, regardless of the code or cross-section library. We could not resolve this large discrepancy. Smaller discrepancies were observed, for example, MCNP5 results were significantly greater for copper and lead by ~23 and 14%

respectively, and smaller for aluminium and iron by ~10 and 9%. COG results were high for graphite and Ta. Discrepancies are probably a combination of differences in cross-section libraries, and code implementations. The last column gives gamma energy leakage for the latest translation of ENDF/B-VII. Results are significantly lower for N_2 and Au, and consistently lower for high Z materials, W, Au, Pb and Th-232. In any case, these simple tests already proved very useful for the V&V of the latest LLNL translations, and to detect bugs in the cross-section library itself (see titanium).

Table II: Simulated Gamma-ray MeV per 14 MeV neutron (γ MeV/n)

		TART		[γ MeV/n]/[C/E] *		COG	MCNP5	Mercury
Material	rho.R * (g/cm2)	ENDL (1988)	ENDF/B-V (1987)	ENDL (1988)	ENDF/B-V (1987)	ENDF/B-VIr7	ENDF/B-VI	ENDF/B-VII.0
Carbon	40	0.9	0.85	0.99	1.03	0.950	0.847	0.895
Nitrogen	40	1.35	1.14	1.38	1.46	1.193	1.196	1.114
H2O	25	0.93	0.71	0.81	0.87	1.359	1.472	1.397
C2F4	35	0.98	0.61	0.72	0.69	0.633	0.609	0.565
Al	35	1.97	1.58	1.88	1.98	1.409	1.425	1.418
Si	35	2.15	1.67	2.00	2.26	1.664	1.679	1.603
Ti	45	1.44	1.53	1.84	1.68	1.510	1.531	X
Fe	40	1.49	1.25	1.37	1.49	1.188	1.139	1.183
Cu	45	0.89	0.99	0.91	0.93	0.883	1.215	0.870
Ta	35	0.51	0.43	*0.56*	*0.55*	*0.789*	0.401	0.355
W	35	0.42	0.39	0.52	0.48	0.378	0.373	0.365
Au	40	0.33		0.35		0.341	0.340	0.333
Pb	35	0.35	0.29	0.30	0.31	0.277	0.251	0.199
Th232	35	0.34	0.29	0.35	0.34	0.291	0.291	0.234
U238	35	0.38	0.32	0.37	0.38	0.333	0.341	0.328

* C/E is a correction factor

6. Conclusion and Future Work

A set of models of the LLNL pulsed-sphere benchmark experiments have been developed that allows to test newly evaluated cross-sections by comparing neutron leakage to measurements, and gamma leakage to TART simulations.

Acknowledgements

Special thanks to the Mercury team, in particular Richard ”Spike” Procassini, Scott McKinley, for enhancing the code to help me set-up these benchmark simulations, and for their patience answering my questions about Mercury.

References:

1. Wong C., Anderson J.D., Brown P., Hansen L.F., Kammerdiener J.L., Logan C., and Pohl B., Livermore Pulsed Sphere Program: Program Summary through July 1971, UCRL-51144, Rev. 1, (1972).

2. Marchetti A. and G. W. Hedstrom, "New Monte Carlo Simulations of the LLNL Pulsed Sphere Experiments," Lawrence Livermore National Laboratory report, UCRL-ID-131461 (1998).

3. Van der Marck S. C., “BenchmarkingENDF/B.VII.0,” Nuclear Data Sheet, 107, 3061-3118 (2006).

4. Goldberg E., Hansen L.F., Komoto T. T., Pohl B. A., Howerton R. J., Dye R. E., Plechaty E. F., and W E Warren, " neutron and gamma-ray spectra from a variety of materials bombarded with 14-MeV neutrons," Nucl. Sci Eng., 105, 319 (1990).

5. Hansen L F., Wong C., Komoto T. T., Pohl B. A., Goldberg E., Howerton R. J., Webster W. M., "Neutron and gamma spectra from 232Th, 23 'U, 238U, and 239pu after bombardment with 14 MeV neutrons," Nucl. Sci. Eng. 72, 35 (1979).

6. Hansen L. F., Goldberg E., Howerton R. J., Komoto T. T., and Pohl B. A., Updated Summary of Measurements and Calculations of Neutron and Gamma-Ray Emission Spectra from Spheres Pulsed with 14-MeV Neutrons, Lawrence Livermore National Laboratory, Report UCID-19604, Rev 1, (1989).

7. MERCURY User Guide version b.15, LLNL Technical manual, UCRL-TM-204296, Rev.1, (2006).

8. Chadwick M.B., Obložinský P., HermanM., Greene N.M., McKnight R.D., Smith D.L., Young P.G., MacFarlane R.E., Hale G.M., Frankle S.C., Kahler A.C., Kawano T., Little R.C., Madland D.G., Moller P., Mosteller R.D., Page P.R., Talou P., Trellue H., White M.C., *et al.* ENDF/B-VII.0: Next Generation Evaluated Nuclear Data Library for Nuclear Science and Technology, 107, 12, 2931-306 (2006)

9. Lent, R. M. Buck, E. M.T. Wilcox, S. Hadjimarkos, "COG A Multiparticle Monte Carlo Transport Code User's Manual," Fifth Edition Lawrence Livermore National Laboratory, Livermore, California, UCRL-TM-202590 (2002).

10. Frankle S., Possible impact of additional collimators on the LLNL pulsed-sphere experiments (U) LA-UR-05-5877, X-5:SCF-04-004(U) (2004).

11. Frankle S., LLNL pulsed-sphere measurements and detector response functions (U) LA-UR-05-5878, X-5:SCF-04-001(U) (2004).

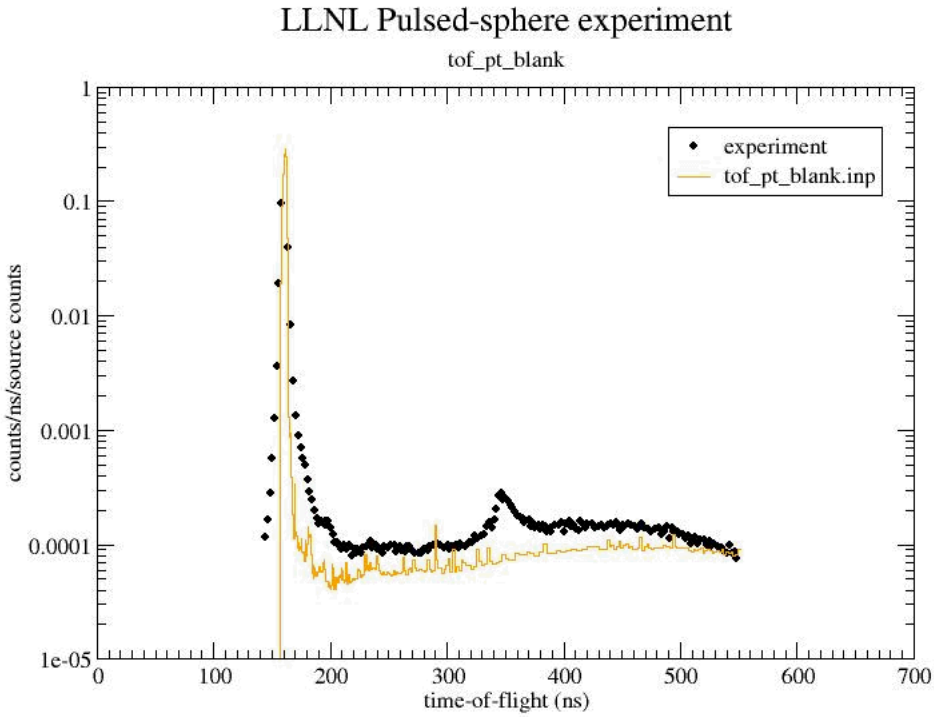

Figure 1. Neutron TOF spectra for the LLNL pulsed-sphere: blank run
Measured spectrum (black dot), Mercury simulation (orange)

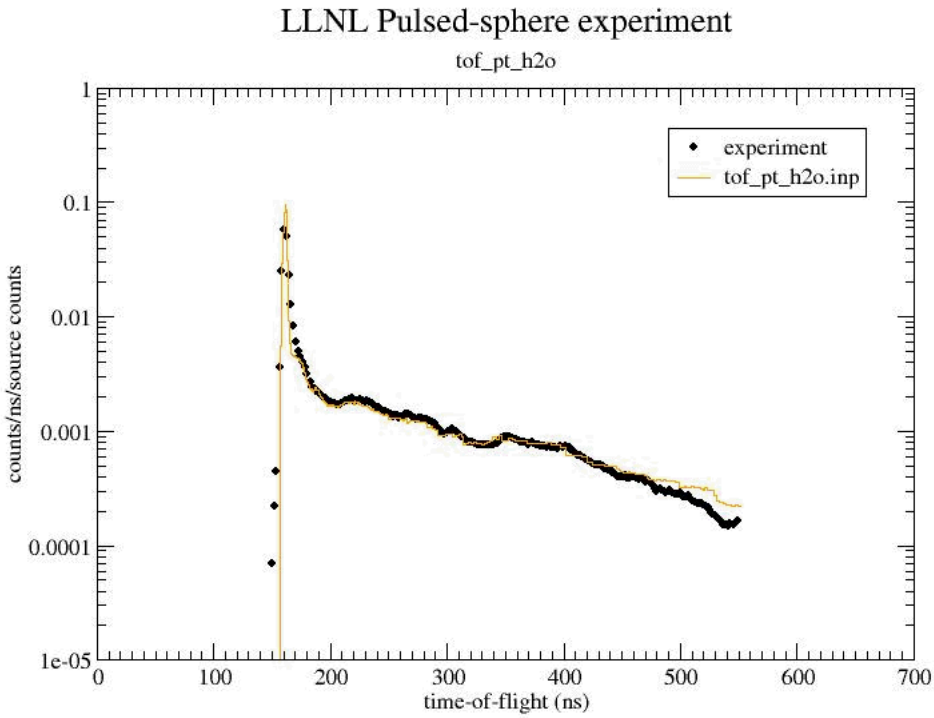

Figure 2. Neutron TOF spectra for the LLNL pulsed-sphere: water
Measured spectrum (black dot), Mercury simulation (orange)

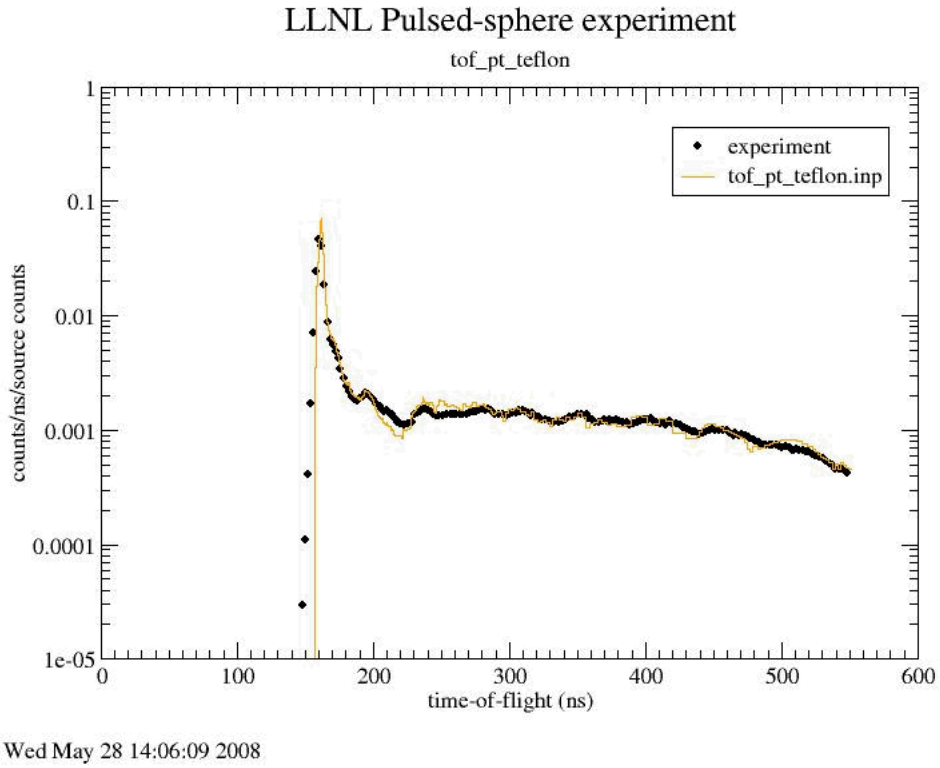

Figure 3. Neutron TOF spectra for the LLNL pulsed-sphere: Teflon

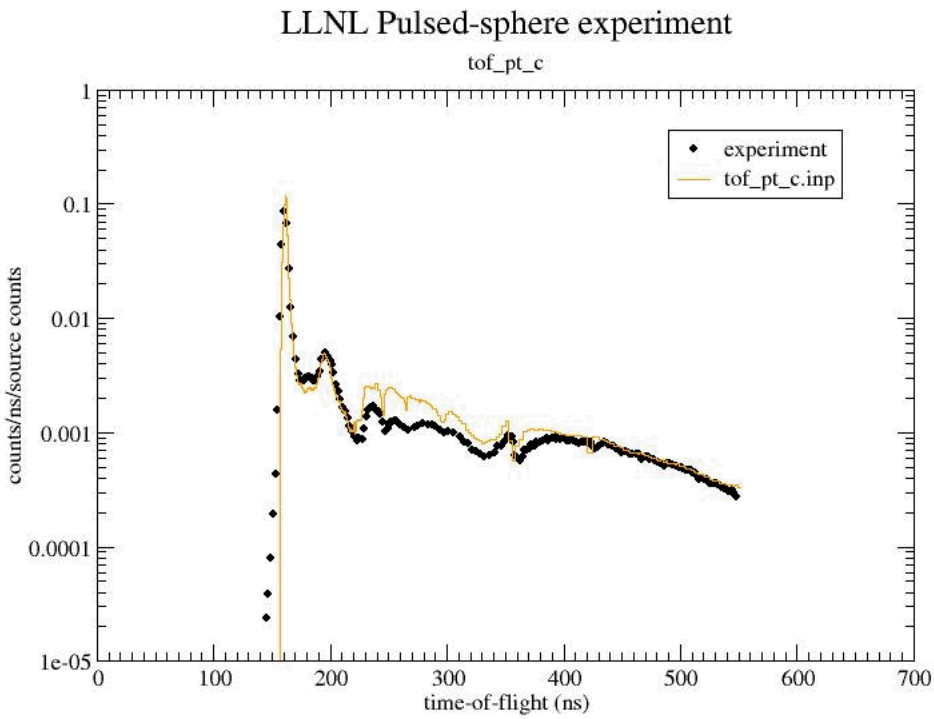

Figure 4. Neutron TOF spectra for the LLNL pulsed-sphere: graphite

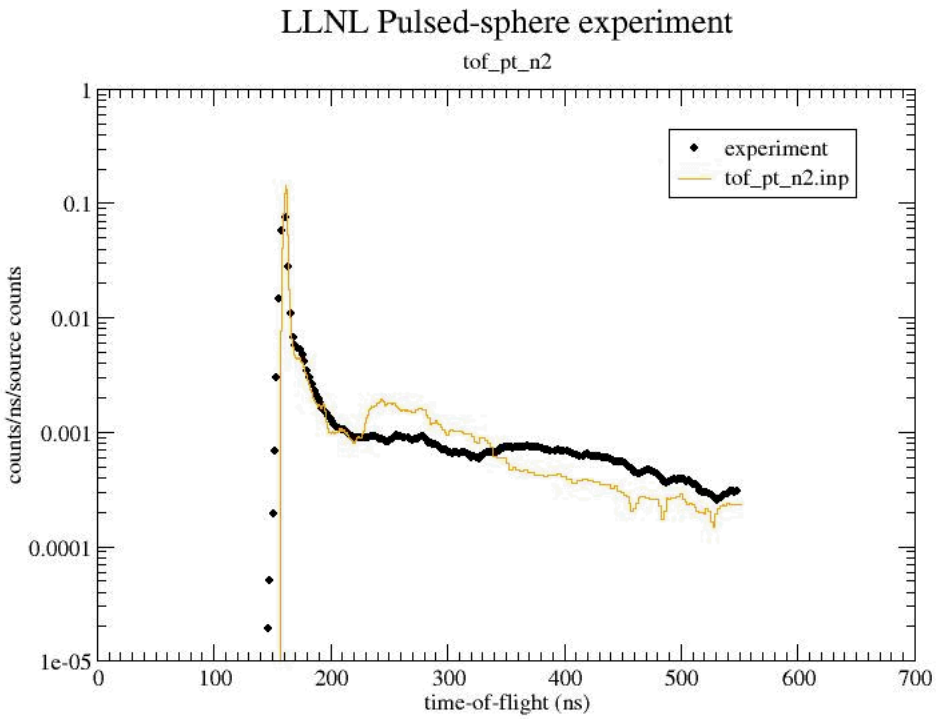

Figure 5. Neutron TOF spectra for the LLNL pulsed-sphere: nitrogen

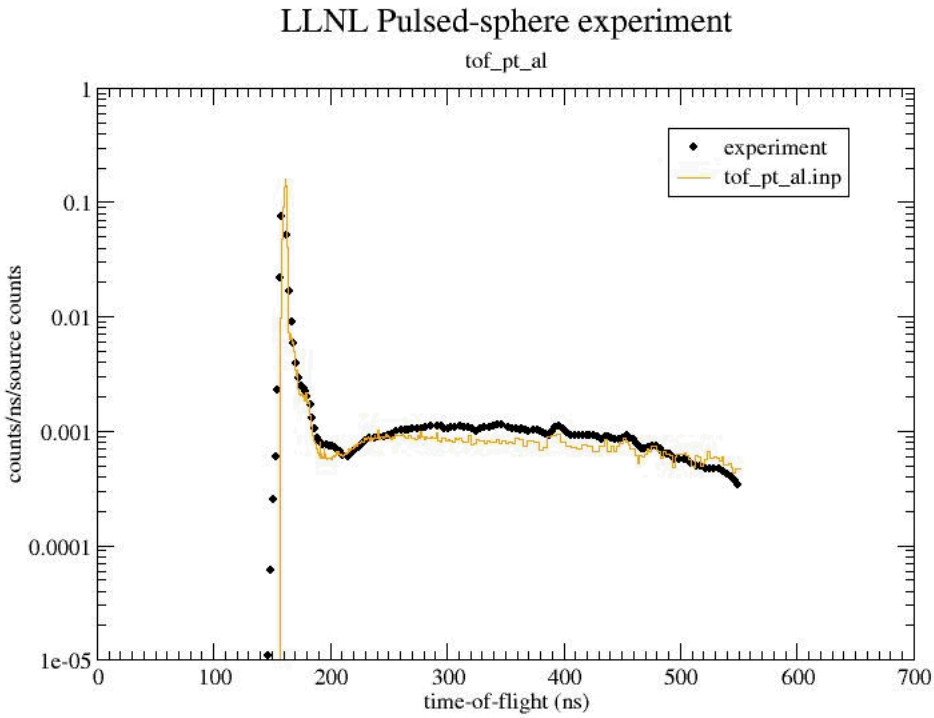

Figure 6. Neutron TOF spectra for the LLNL pulsed-sphere: Al

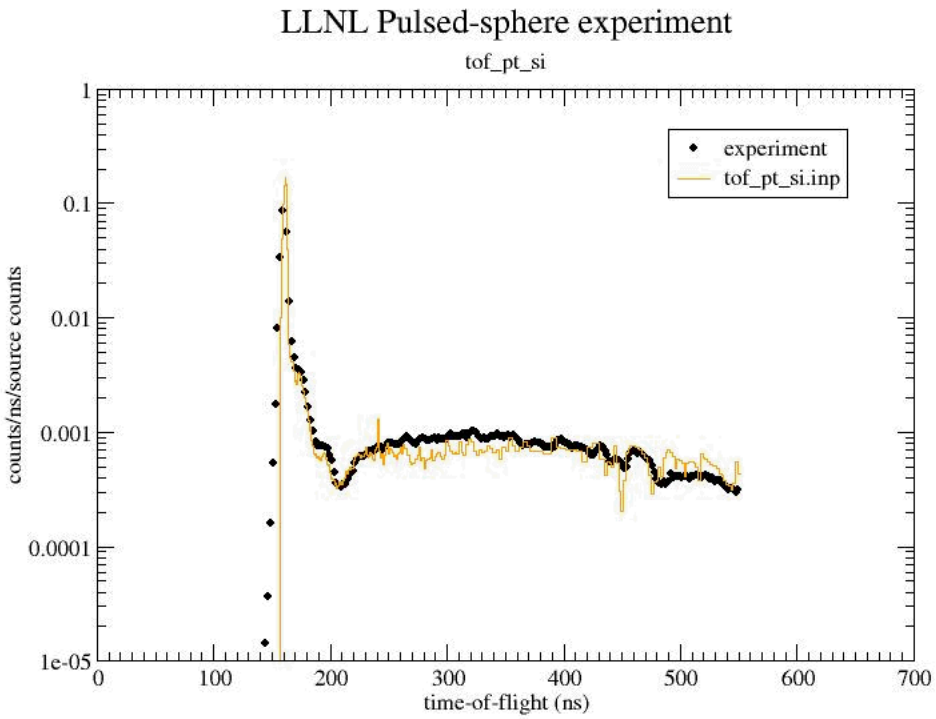

Figure 7. Neutron TOF spectra for the LLNL pulsed-sphere: Si

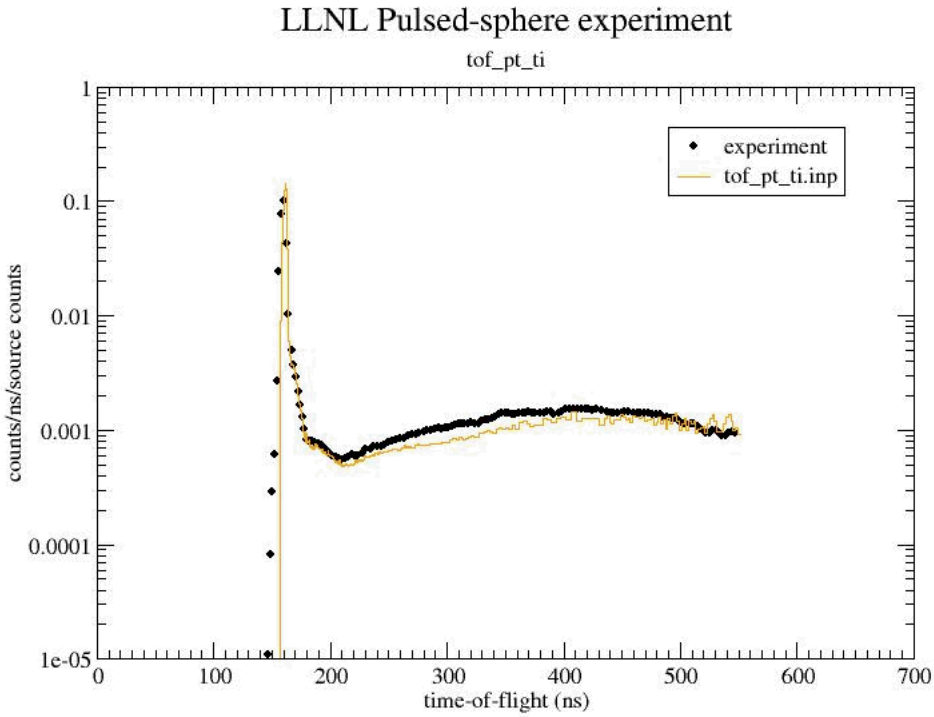

Figure 8. Neutron TOF spectra for the LLNL pulsed-sphere: Ti

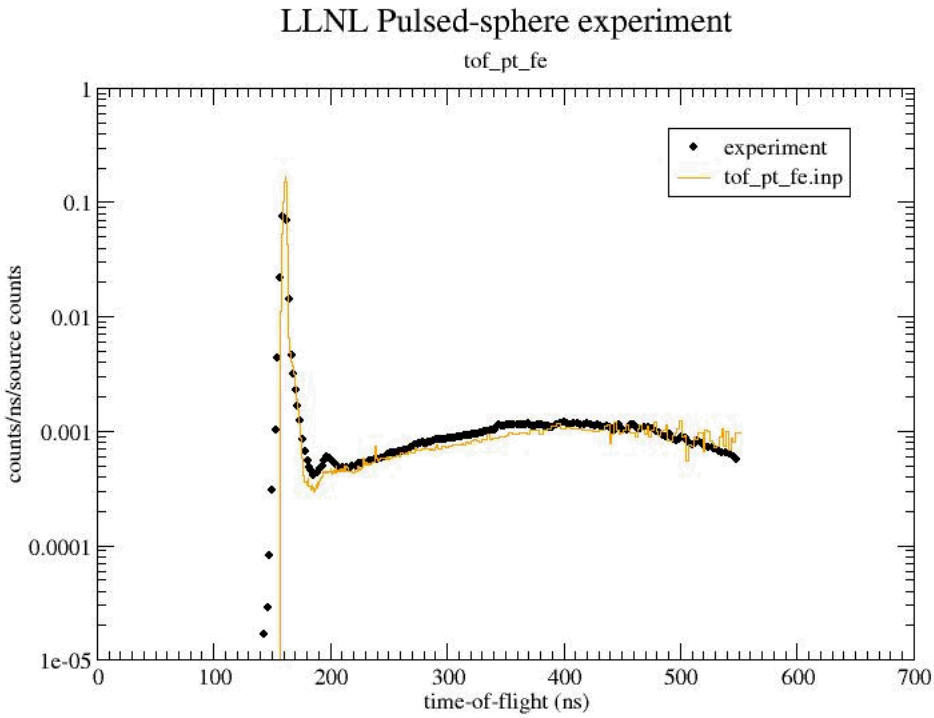

Figure 9. Neutron TOF spectra for the LLNL pulsed-sphere: Fe

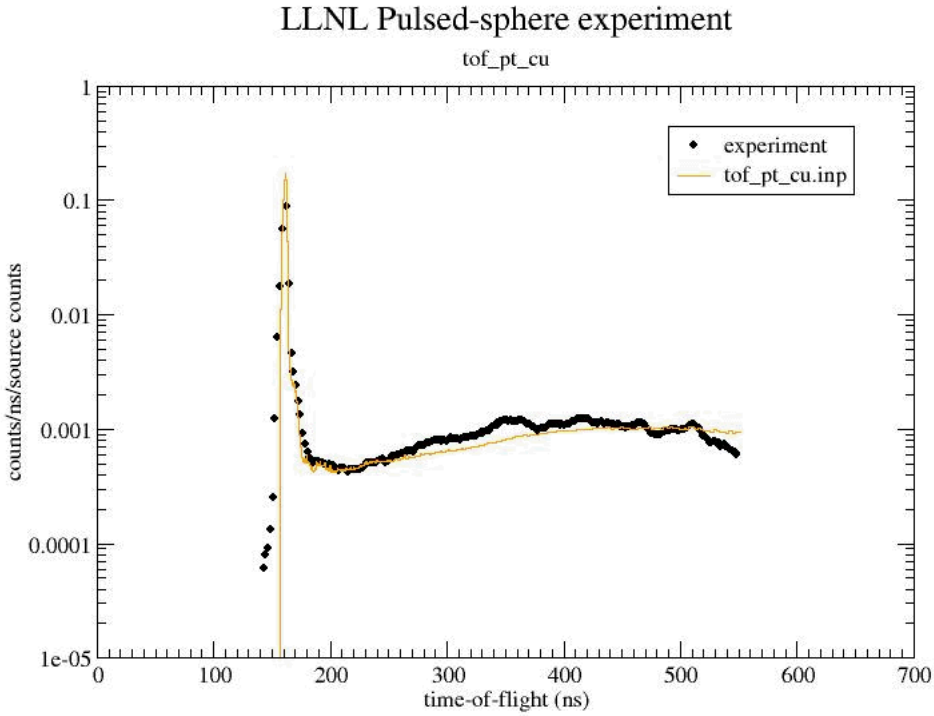

Figure 10. Neutron TOF spectra for the LLNL pulsed-sphere: Cu

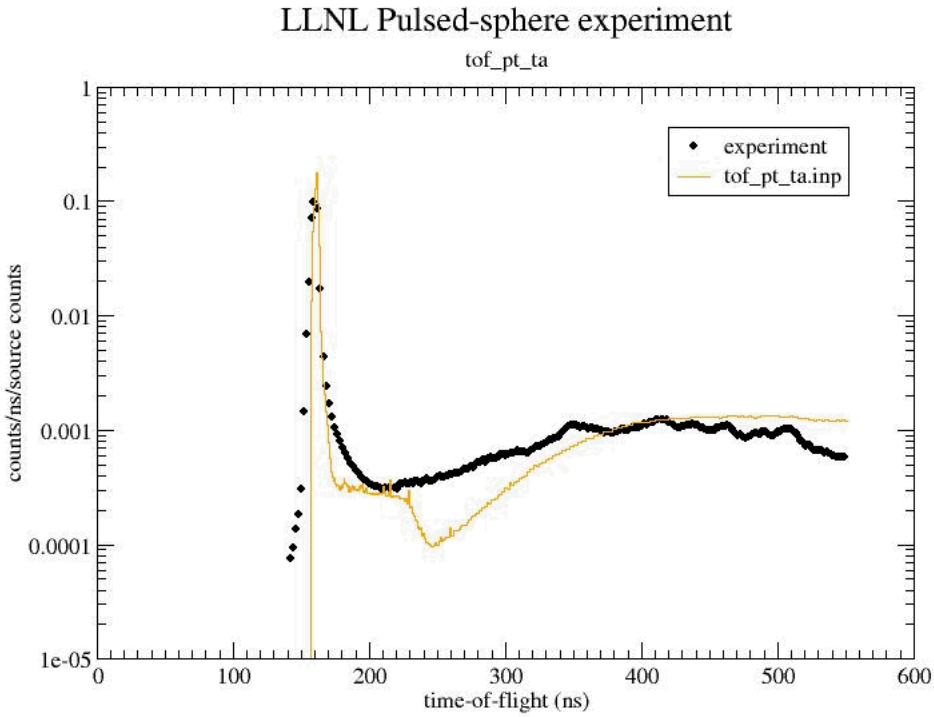

Figure 11. Neutron TOF spectra for the LLNL pulsed-sphere: Ta

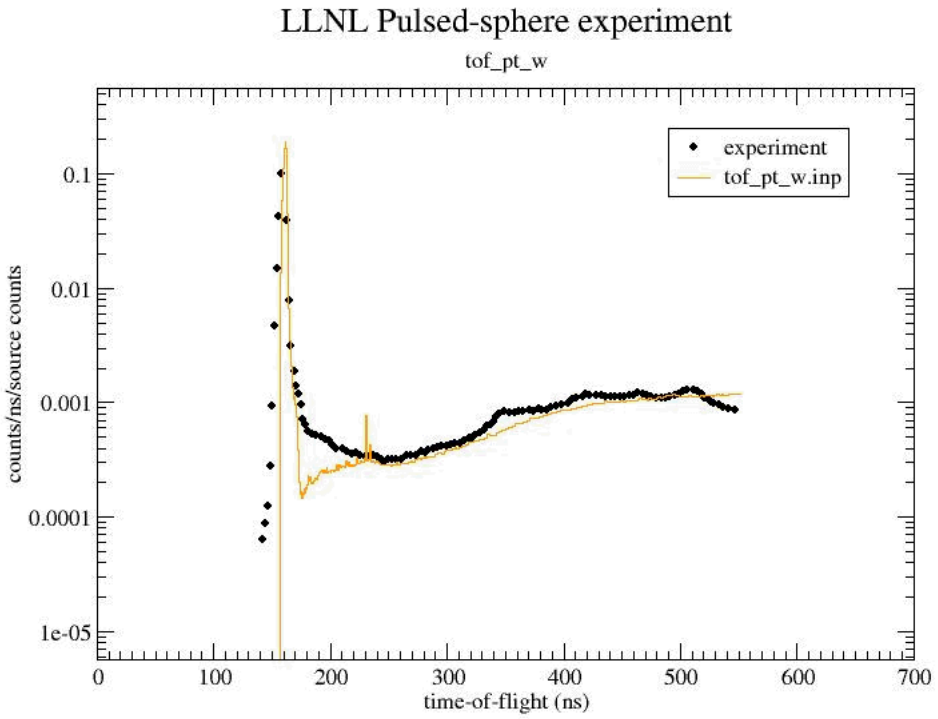

Figure 12. Neutron TOF spectra for the LLNL pulsed-sphere: W

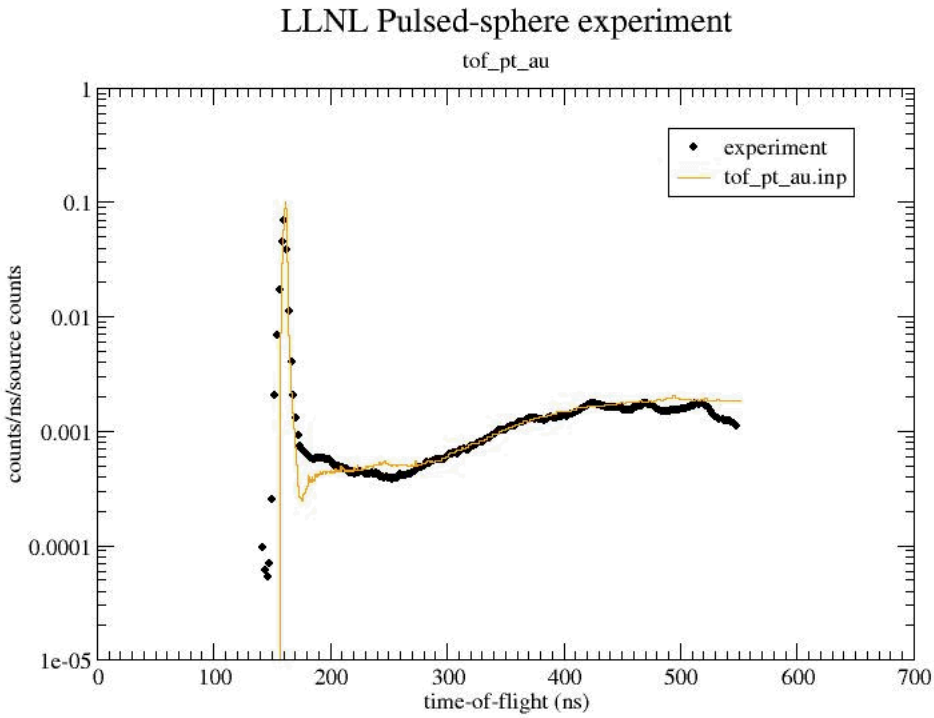

Figure 13. Neutron TOF spectra for the LLNL pulsed-sphere: Au

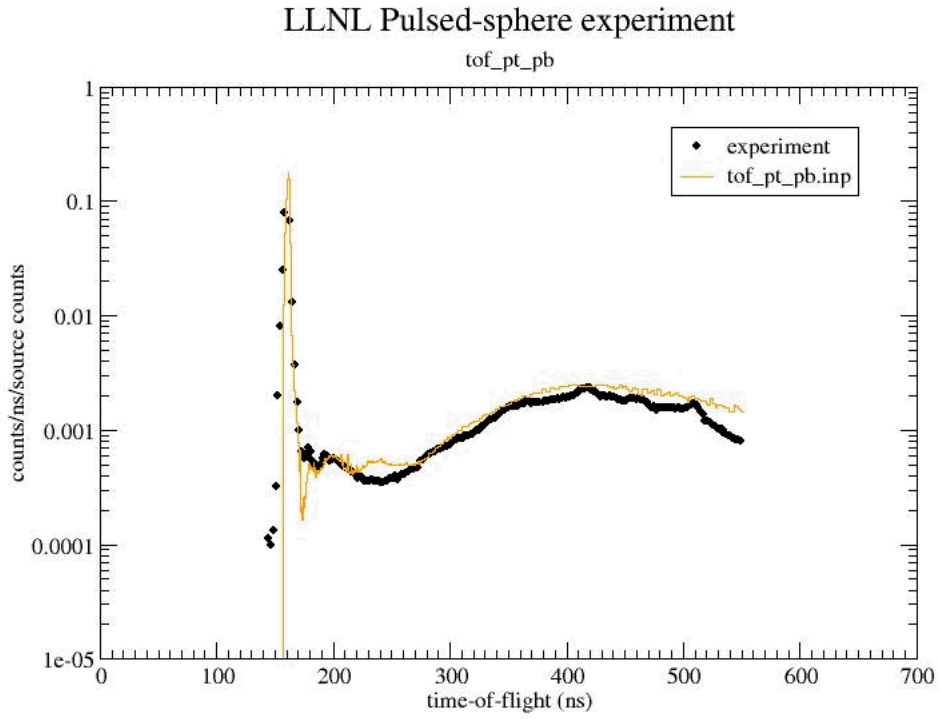

Figure 14. Neutron TOF spectra for the LLNL pulsed-sphere: Pb

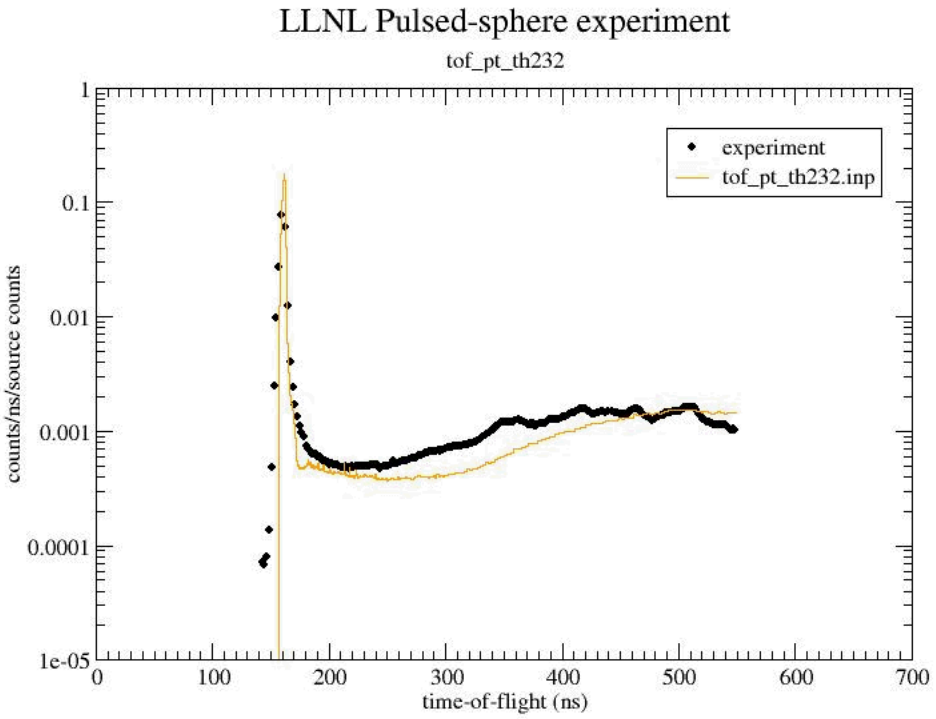

Figure 15. Neutron TOF spectra for the LLNL pulsed-sphere: ^{232}Th

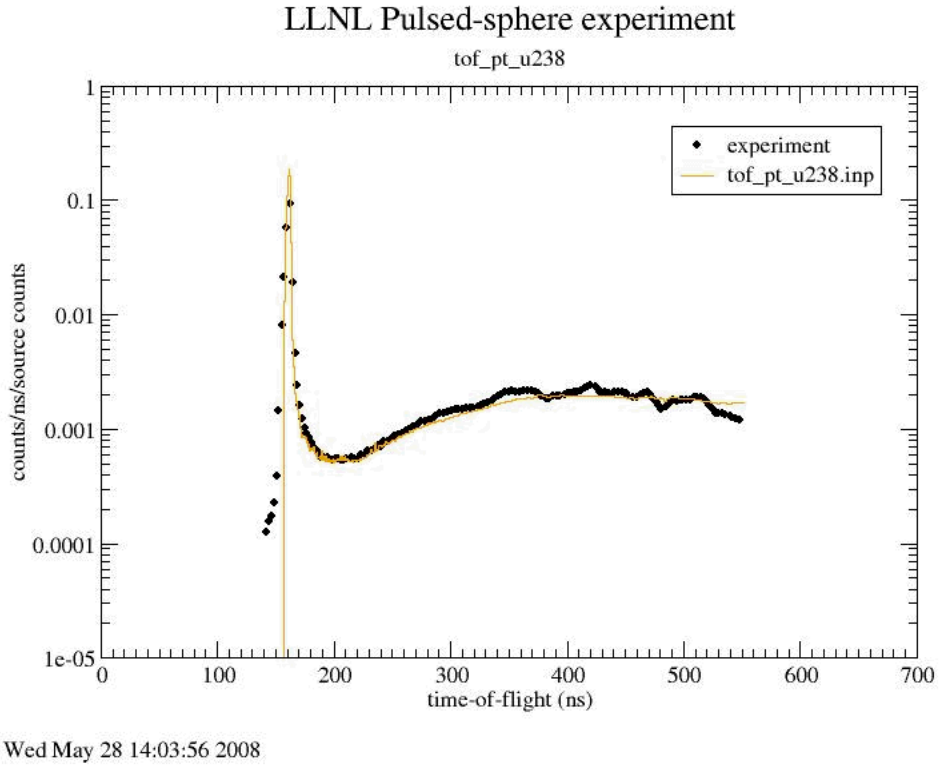

Figure 16. Neutron TOF spectra for the LLNL pulsed-sphere: ^{238}U

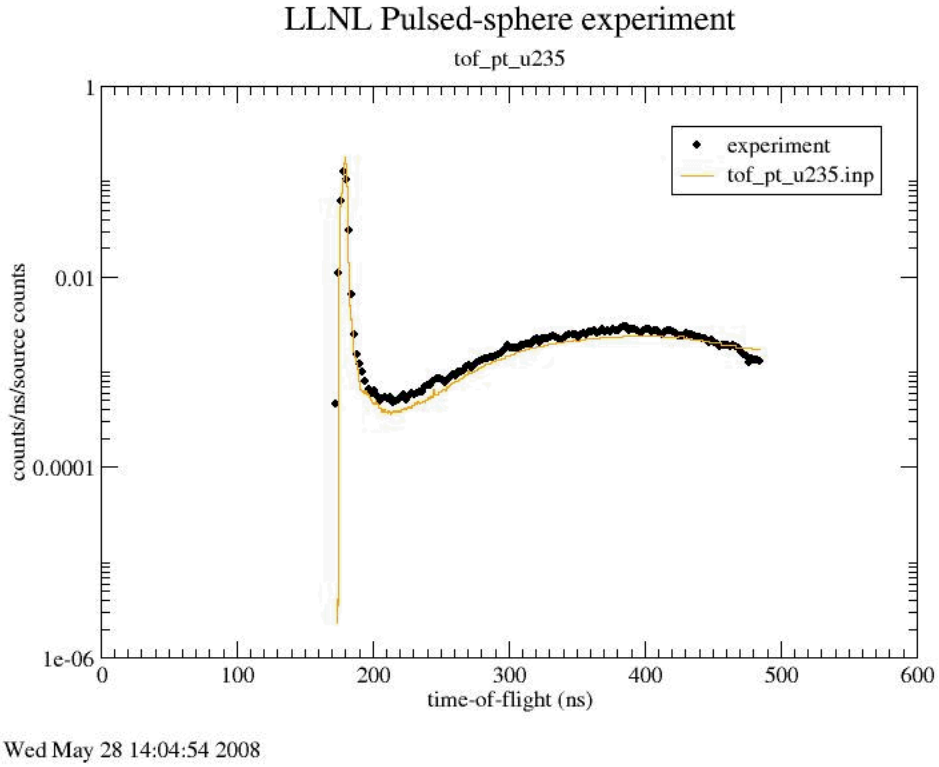

Figure 17. Neutron TOF spectra for the LLNL pulsed-sphere: ^{235}U

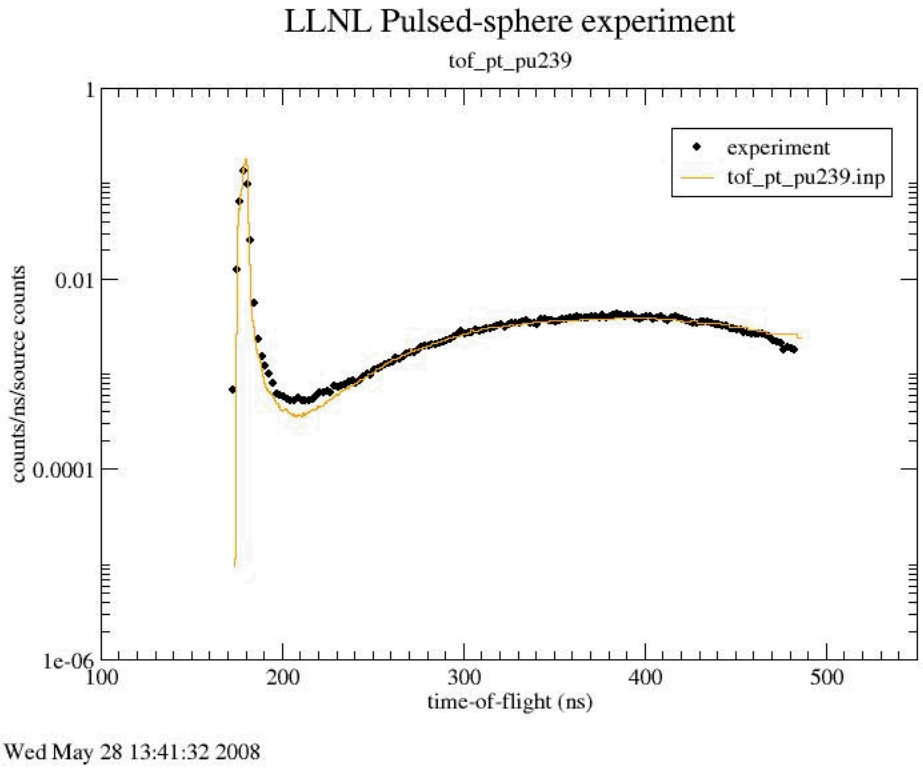

Figure 18. Neutron TOF spectra for the LLNL pulsed-sphere: ^{239}Pu